Journal of Power Sources 196 (2011) 3342–3345

Contents lists available at ScienceDirect

Journal of Power Sources

journal homepage: www.elsevier.com/locate/jpowsour

Short communication

High lithium ionic conductivity in the garnet-type oxide $Li_{7-X}La_3(Zr_{2-X}, Nb_X)O_{12}$ ($X = 0–2$)

Shingo Ohta*, Tetsuro Kobayashi, Takahiko Asaoka

Toyota Central R&D Labs. Inc., Battery & Cells Div., 41-1 Yokomichi, Nagakute, Aichi 480-1192, Japan

ARTICLE INFO

Article history:
Received 1 September 2010
Received in revised form 2 November 2010
Accepted 10 November 2010
Available online 24 November 2010

Keywords:
Solid electrolytes
All-solid-state lithium battery
Oxides
Ceramics
Lithium ion conductivity

ABSTRACT

Lithium garnet-type oxides $Li_{7-X}La_3(Zr_{2-X}, Nb_X)O_{12}$ ($X = 0–2$) were synthesized by a solid-state reaction, and their lithium ion conductivity was measured using an AC impedance method at temperatures ranging from 25 to 150 °C in air. The lithium ion conductivity increased with increasing Nb content, and reached a maximum of ~0.8 mS cm^{-1} at 25 °C. By contrast, the activation energy reached a minimum of ~30 kJ mol^{-1} at the same point with $X = 0.25$. The potential window was examined by cyclic voltammetry (CV), which showed lithium deposition and dissolution peaks around 0 V vs. Li^+/Li, but showed no evidence of other reactions up to 9 V vs. Li^+/Li.

1. Introduction

Recently, high-power, high-capacity lithium ion batteries are in strong demand for use in electric vehicles and load-leveling applications, such as wind-generated electricity and photovoltaic cells. Safer lithium ion batteries will inevitably be required. All-solid-state lithium ion batteries containing solid electrolytes are considered to be safer than lithium ion batteries that use liquid organic electrolytes, and all-solid-state lithium ion batteries have attracted great attention. In order to improve the performance of all-solid-state lithium ion secondary batteries, new solid electrolytes are required with the following properties: (1) a high lithium ionic conductivity, with a negligible electron contribution (conduction), (2) stability against chemical reaction with lithium at the anode, and Co-, Ni-, or Mn-containing oxides at the cathode, and (3) a wide electrochemical window allowing the use of high-voltage cathode materials (≥5 V vs. Li^+/Li) and lithium metal anodes. Oxide materials are believed to potentially have advantages over other inorganic materials in terms of their handling and chemical stability. The glassy lithium phosphorus oxynitride (LiPON) [1] was proposed for use in a thin-film solid-state lithium ion battery, and was confirmed to function as a solid-state electrolyte [2]. However, the low power density of solid-state lithium ion batteries using LiPON was considered disadvantageous due to the low lithium ion conductivity of LiPON (~1 μS cm^{-1} at room temperature). Some oxide materials, such as perovskite-type oxides (Li, La)TiO_3 [3,4] or NASICON-type structured oxides, e.g., $LiTi_2P_3O_{12}$ [5], and their derivatives [6], exhibit high lithium ion conductivity (~1 mS cm^{-1} at room temperature) but are not yet applicable as electrolytes in lithium ion batteries because they allow lithium insertion to reduce Ti^{4+} to Ti^{3+} around 1.5 V vs. Li^+/Li. To date, no oxide material has been reported to have both a high lithium ion conductivity and a wide electrochemical window.

Recently, the lithium garnet-type oxide $Li_7La_3Zr_2O_{12}$, which was discovered by Thangadurai and Weppner in 2007 [7], was seen as a promising candidate solid electrolyte because it has a high chemical stability and a wide potential window. However, the lithium ion conductivity of $Li_7La_3Zr_2O_{12}$ is ~0.2 mS cm^{-1} at room temperature, about two orders of magnitude lower than that of a common liquid organic electrolyte. Hence, it is necessary to improve the lithium ion conductivity of this compound. It is well known that lithium ion conductivity strongly depends on the lattice parameter in other lithium garnet-type oxides, as observed in $Li_5La_3M_2O_{12}$ (M = Nb, Ta) after the substitution of alkali earth elements for the lanthanum site [8–12]. Therefore, an appropriate structural modification should increase the lithium ion conductivity of lithium garnet-type oxides. Here, we report the successful improvement of the lithium ion conductivity of $Li_7La_3Zr_2O_{12}$ by substitutional Nb-doping.

2. Experimental

$Li_{7-X}La_3(Zr_{2-X}, Nb_X)O_{12}$ ($X = 0–2$) bulk ceramic samples were fabricated by conventional solid-state reaction. The starting mate-

* Corresponding author. Tel.: +81 561 71 7659; fax: +81 561 63 5743.
E-mail address: sohta@mosk.tytlabs.co.jp (S. Ohta).

0378-7753/$ – see front matter © 2010 Elsevier B.V. All rights reserved.
doi:10.1016/j.jpowsour.2010.11.089

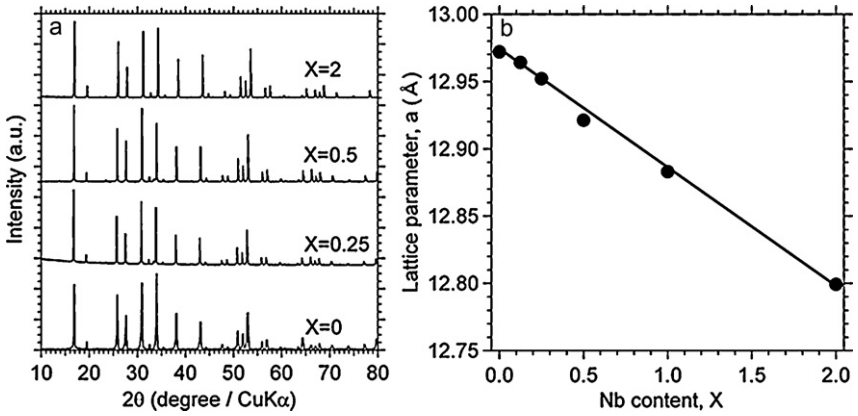

Fig. 1. (a) XRD patterns of $Li_{7-X}La_3(Zr_{2-X}, Nb_X)O_{12}$ ($X = 0$–2) samples. (b) Change in the lattice parameter of $Li_{7-X}La_3(Zr_{2-X}, Nb_X)O_{12}$ as a function of Nb content. The solid line is shown as a visual guide.

rials, Li_2CO_3 (10% excess was added to account for the evaporation of lithium at high temperatures) $La(OH)_3$, ZrO_2, and Nb_2O_5, were mixed by planetary ball-milling, and then calcinated at 950 °C for 12 h. The calcinated powders were pressed into pellets and sintered at 1200 °C for 36 h. The crystal structure and lattice parameters of the samples were evaluated by X-ray diffraction (XRD) using Cu Kα radiation.

The electrical conductivity of the samples was measured in air using a two-probe AC impedance method with an Agilent 4294A in the frequency range of 40 Hz to 110 MHz at temperatures from 25 to 150 °C. Au electrodes were affixed to both sides of the pellets using Au nano-metal ink (ULVAC Materials, Inc.) for the measurement. (The pellet and ink were heated at 350 °C for 0.5 h.)

The electrochemical windows of the samples were evaluated by cyclic voltammetry (CV) using a potentio-galvanostat (Solartron 1480) at a scanning rate of 1 mV s^{-1} between −0.5 and 9 V (vs. Li^+/Li). An Au electrode and lithium metal were attached to both faces of the pellet as working and counter electrodes, respectively.

3. Results and discussion

Fig. 1(a) shows XRD patterns of the $Li_{7-X}La_3(Zr_{2-X}, Nb_X)O_{12}$ samples. All of the observed diffraction peaks were indexed as a cubic lithium garnet-like structure (space group: *Ia*−*3d*) [13]. Lattice parameters of the $Li_{7-X}La_3(Zr_{2-X}, Nb_X)O_{12}$ samples calculated from their XRD patterns are shown in Fig. 1(b). The Lattice parameter of $Li_{7-X}La_3(Zr_{2-X}, Nb_X)O_{12}$ decreased linearly with increasing Nb-content (X) according to Vegard's law, indicating that Nb^{5+} (86.0 pm) was substituted at Zr^{4+} (70.9 pm) sites [14].

Fig. 2 shows a Nyquist plot of $Li_{6.75}La_3Zr_{1.75}Nb_{0.25}O_{12}$ at 25 °C in air. The plot can be well-resolved into bulk, grain-boundary, and electrode resistances. The semicircle in the high-frequency region represents the bulk resistance, and the other one represents the grain-boundary resistance. The appearance of a tail at the low-frequency region suggests that the electrode blocked mobile lithium ions. The solid line in Fig. 2 represents fitted data based on an equivalent circuit model consisting of two parallel resistance (R) and capacitance (C) contributions $(R_bC_b)(R_{gb}C_{gb})(R_{el})$, where b, gb, and el denote the bulk, grain-boundary, and electrode, respectively. The values of R_b and R_{gb} at 25 °C were 211 Ω cm^2 and 49 Ω cm^2, respectively (sample size: 13 mmØ, 2 mm^t). The grain boundary contribution to the total resistance ($R_{gb}/(R_b + R_{gb})$) was ∼20%, which is comparable to that of any other family of lithium garnet-type oxides [8–11]. The Nyquist plots of $Li_{7-X}La_3(Zr_{2-X}, Nb_X)O_{12}$ remained constant for a week, independent of exposure time in air at room temperature, demonstrating the stability of $Li_{7-X}La_3(Zr_{2-X}, Nb_X)O_{12}$ at room temperature in air.

The temperature dependence of the total (bulk plus grain-boundary) lithium ion conductivity of $Li_{7-X}La_3(Zr_{2-X}, Nb_X)O_{12}$ is shown in Fig. 3(a). The lithium ion conductivity was linear and obeyed the Arrhenius law ($\sigma = A\exp(-E_a/kT)$, where A is the frequency factor, k is the Boltzmann constant, T is the absolute temperature, and E_a is the activation energy, indicating that no structure or phase changes occurred in the observed temperature range. The lithium ion conductivity at 25 °C and the activation energy are plotted in Fig. 3(b). The lithium ion conductivity increased with X, reaching a maximum of 0.8 mS cm^{-1} at $X = 0.25$, which is comparable to the behavior of other fast lithium ion conducting oxides, such as NASICON-type oxides [5,6]. In contrast, the activation energy reached a minimum value of ∼30 kJ mol^{-1} at the same value of $X = 0.25$. Although the lithium ion conductivity was previously reported to increase proportionally with the lattice parameter in other lithium garnet-type oxides [8–11], the lithium ion conductivity of $Li_{7-X}La_3(Zr_{2-X}, Nb_X)O_{12}$ showed no significant dependence on the lattice parameter. Therefore, the lithium ion conduction characteristics of lithium garnet-type oxides cannot be explained as a function of lattice parameter alone. The density of the sintered pellets varied between 89 and 92% of the theoretical value calculated from the lattice parameter. The grain-boundary contribution to the total resistance shows no significant dependence on Zr/Nb ration ($R_{gb}/(R_b + R_{gb})$, $Li_7La_3Zr_2O_{12}$: 12%, $Li_{6.75}La_3(Zr_{1.75}, Nb_{0.25})O_{12}$: 20%, and $Li_5La_3Nb_2O_{12}$: 28% respectively). Therefore, the variation of lithium ion conductivity and activation energy with Nb content (X) was not due to the influence of density. There are two factors for improving the ionic conductivity; (i) to increase

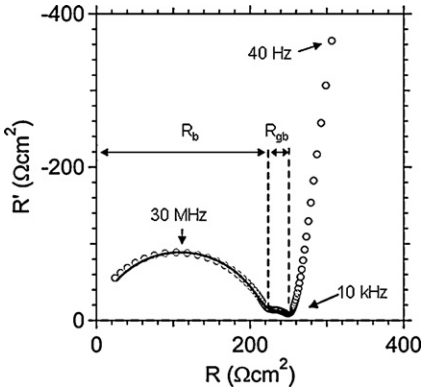

Fig. 2. Nyquist plot (40 Hz to 110 MHz) of $Li_{6.75}La_3Zr_{1.75}Nb_{0.25}O_{12}$ at 25 °C in air using Au electrodes. The solid line represents fitted data based on an equivalent circuit model consisting of two resistances and capacitances, representing the bulk and the grain boundary.

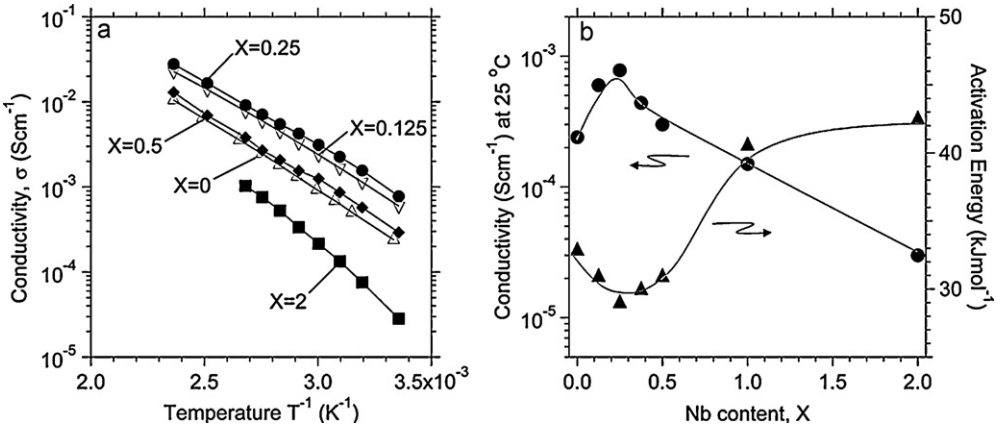

Fig. 3. (a) Temperature dependence of lithium ion conductivity of $Li_{7-X}La_3(Zr_{2-X}, Nb_X)O_{12}$ ($X = 0$–2) samples. (b) Lithium ion conductivity at 25 °C and activation energy as a function of Nb content. The solid lines are provided as visual guides.

the carrier concentration; (ii) to increase the carrier mobility. In this case, lithium concentration (n) calculated from the lattice parameter between $Li_7La_3Zr_2O_{12}$ and $Li_{6.75}La_3(Zr_{1.75}, Nb_{0.25})O_{12}$ was almost same (n of $Li_7La_3Zr_2O_{12}$ and $Li_{6.75}La_3(Zr_{1.75}, Nb_{0.25})O_{12}$ was $2.49 \times 10^{22}\,cm^{-3}$ and $2.42 \times 10^{22}\,cm^{-3}$). Thus, it should be considered that an increase in carrier lithium mobility due to Nb-substitutional doping lead to the enhancement of lithium ion conductivity.

Recently, in order to clarify the lithium ion conducting mechanism in lithium garnet-type oxides, a detailed evaluation of the structure of other lithium garnet-type oxides, $Li_5La_3M_2O_{12}$ (M = Nb, Ta), was reported on the basis of neutron powder diffraction measurements [15,16]. Lithium in these garnet-like structures occupied tetrahedral sites (24 d) and distorted octahedral sites (96 h), indicating that the lithium ion conduction pathway was composed between these sites. Therefore, we believe that the enhancement of lithium ion conductivity in lithium garnet-type oxides is caused by a structural modification around the lithium sites and is not entirely due to an increase in the lattice parameter. In order to determine the reasons for lithium ion conductivity enhancement due to Nb-substitutional doping, studies on the changes in the lithium ion conduction pathway in $Li_{7-X}La_3(Zr_{2-X}, Nb_X)O_{12}$ using neutron powder diffraction measurements are currently in progress.

A cyclic voltammogram of $Li_{6.75}La_3(Zr_{1.75}, Nb_{0.25})O_{12}$ is shown in Fig. 4, which reveals lithium deposition and dissolution peaks near 0 V vs. Li^+/Li, but indicates no other reactions up to 9 V vs. Li^+/Li.

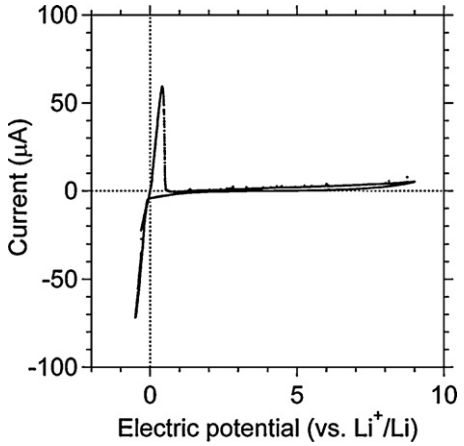

Fig. 4. A cyclic voltammogram of $Li_{6.75}La_3(Zr_{1.75}, Nb_{0.25})O_{12}$ bulk ceramic, recorded at a scanning rate of 1 mV s^{-1} at 25 °C.

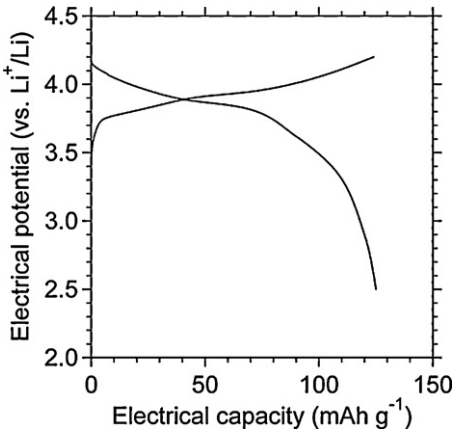

Fig. 5. Charge-discharge curve of $LiCoO_2/Li_{6.75}La_3(Zr_{1.75}, Nb_{0.25})O_{12}$/Li battery. The horizontal axis shows the capacity normalized by the weight of the $LiCoO_2$ cathode.

Therefore, $Li_{6.75}La_3(Zr_{1.75}, Nb_{0.25})O_{12}$ has a wide electrochemical window.

In order to assess the feasibility of using $Li_{6.75}La_3(Zr_{1.75}, Nb_{0.25})O_{12}$ as a solid electrolyte material for all-solid-state lithium ion batteries, we constructed an all-solid-state lithium ion battery using $Li_{6.75}La_3(Zr_{1.75}, Nb_{0.25})O_{12}$ (solid electrolyte), lithium (anode), and $LiCoO_2$ (cathode). $LiCoO_2$ was deposited by pulsed laser deposition (PLD) on the top side of the sintered $Li_{6.75}La_3(Zr_{1.75}, Nb_{0.25})O_{12}$ pellet. On the bottom of the pellet, a lithium metal foil was attached as the anode. Fig. 5 shows charge-discharge curves of this battery at 25 °C. The current density was 3.5 μA cm^{-2} and the charge-discharge Coulombic efficiency was nearly 100%. The plateau of charge curves starts at approximately 3.7 V, which is slightly lower than the conventional extraction/insertion reaction of $LiCoO_2$ (3.9 V) due to the lower crystallinity of $LiCoO_2$ prepared by PLD. The theoretical electrochemical capacity of $LiCoO_2$ is 137 mAh g^{-1}, which corresponds to 0.5 Li per CoO_2. The charge and discharge capacities of this battery were 125 mAh g^{-1}, which corresponded to about 90% of the theoretical capacity. This result is the first indication that garnet-type oxides are suitable for use as a solid electrolyte material for all-solid-state batteries, and $Li_{6.75}La_3(Zr_{1.75}, Nb_{0.25})O_{12}$ is demonstrated as a promising material for the solid electrolyte of all-solid-state lithium ion batteries.

4. Conclusions

We synthesized substitutionally Nb-doped $Li_7La_3Zr_2O_{12}$ ($Li_{7-X}La_3(Zr_{2-X}, Nb_X)O_{12}$, $X = 0$–2) bulk ceramics by solid-state

reaction. All of the samples had a cubic lithium garnet-like structure, and their lattice parameters changed linearly with respect to Nb content, according to Vegard's law. The lithium ion conductivity increased with increasing Nb content, and reached a maximum of $\sim$0.8 mS cm^{-1} at 25 °C. In contrast, the activation energy reached a minimum of $\sim$30 kJ mol^{-1} at the same X value of 0.25, which was comparable to the behavior of other previously discovered fast lithium ion conducting oxides. The cyclic voltammogram contained lithium deposition and dissolution peaks near 0 V vs. Li^+/Li and indicated no other reactions up to 9 V vs. Li^+/Li, demonstrating that $Li_{7-X}La_3(Zr_{2-X}, Nb_X)O_{12}$ has a wide potential window. We constructed an all-solid-state lithium ion battery using $Li_{7-X}La_3(Zr_{2-X}, Nb_X)O_{12}$ as a solid electrolyte and established the favorable charge-discharge behavior of this battery. Our results indicate that $Li_{7-X}La_3(Zr_{2-X}, Nb_X)O_{12}$ is a promising solid electrolyte material for all-solid-state lithium ion batteries.

References

[1] X. Xu, J.B. Bates, G.E. Jellison, F.X. Hart, J. Electrochem. Soc. 144 (1997) 524.
[2] M. Hayashi, M. Takahashi, Y. Sakurai, J. Power Sources 174 (2007) 990.
[3] Y. Inaguma, C. Liquan, M. Itoh, T. Nakamura, T. Uchida, H. Ikuta, W. Wakihira, Solid State Commun. 86 (1993) 689.
[4] H. Kawai, J. Kuwano, J. Electrochem. Soc. 141 (1994) L78.
[5] V. Thangadurai, A.K. Shukla, J. Gropalakrishnan, J. Mater. Chem. 9 (1999) 739.
[6] J. Fu, J. Am. Ceram. Soc. 80 (1997) 1901.
[7] R. Murugan, V. Thangadurai, W. Weppner, Angew. Chem. Int. Ed. 46 (2007) 7778.
[8] V. Thangadurai, W. Weppner, Adv. Funct. Mater. 15 (2005) 107.
[9] V. Thangadurai, W. Weppner, J. Power Sources 142 (2005) 339.
[10] V. Thangadurai, W. Weppner, J. Am. Ceram. Soc. 88 (2005) 411.
[11] R. Murugan, V. Thangadurai, W. Weppner, J. Electrochem. Soc. 155 (2008) A90.
[12] J. Awaka, N. Kijima, H. Hayakawa, J. Akimoto, J. Solid State Chem. 182 (2009) 2046.
[13] H. Hyooma, K. Hayashi, Mater. Res. Bull. 23 (1988) 1399.
[14] R.D. Shannon, Acta Crystallogr. Sect. A: Cryst. Phys. Diffr. Theor. Gen. Crystallogr. 32 (1976) 751.
[15] E.J. Cussen, Chem. Commun. (2006) 412.
[16] J. Percival, P.R. Slater, Solid State Commun. 142 (2007) 355.